

Cyanobacterial weathering in warming periglacial sediments: Implications for nutrient cycling and potential biosignatures

Cansu Demirel-Floyd  | Gerilyn S. Soreghan  | Megan E. Elwood Madden 

School of Geosciences, University of Oklahoma, Norman, OK, USA

Correspondence

Cansu Demirel-Floyd, School of Geosciences, University of Oklahoma, 100 E Boyd Street, Norman, OK 73019, USA.
Email: cansu.demirel@ou.edu

Funding information

National Science Foundation (NSF), Grant/Award Number: 1543344

Abstract

The cryosphere hosts a widespread microbial community, yet microbial influences on silicate weathering have been historically neglected in cold-arid deserts. Here we investigate bioweathering by a cold-tolerant cyanobacteria (*Leptolyngbya glacialis*) via laboratory experiments using glaciofluvial drift sediments at 12°C, analogous to predicted future permafrost surface temperatures. Our results show threefold enhanced Si weathering rates in pre-weathered, mixed-lithology Antarctic biotic reactors compared to abiotic controls, indicating the significant influence of microbial life on weathering. Although biotic and abiotic weathering rates are similar in Icelandic sediments, neo-formed clay and Fe-(oxy)hydroxide minerals observed in association with biofilms in biotic reactors are common on Icelandic mafic minerals, similar to features observed in unprocessed Antarctic drifts. This suggests that microbes enhance weathering in systems where they must scavenge for nutrients that are not easily liberated via abiotic pathways; potential biosignatures may form in nutrient-rich systems as well. In both sediment types we also observed up to fourfold higher bicarbonate concentrations in biotic reactors relative to abiotic reactors, indicating that, as warming occurs, psychrotolerant biota will enhance bicarbonate flux to the oceans, thus stimulating carbonate deposition and providing a negative feedback to increasing atmospheric CO₂.

KEY WORDS

Antarctic dry valleys, biosignature, cyanobacteria, glacial, Mars, silicate weathering

1 | INTRODUCTION

Occupying 10% of the Earth's land surface and comprising 90% of the cryosphere, the Antarctic continent is a climatically sensitive environment that has major influences on global biogeochemical cycles.^{1,2} This environment is also experiencing some of the most extreme effects of anthropogenic climate change.^{3,4} Increased mean annual temperatures of 3.4°C over the past 50 years resulted in melting ice sheets, unusual flooding events in the McMurdo Dry Valley (MDV) streams and lakes,⁵ retreat of alpine glaciers,⁶ expanding hyporheic zones,⁷ thickening active layer,^{8,9} permafrost loss,¹⁰ and similar changes.³ Whereas current mean annual soil temperatures range between -15°C and -40°C, surface temperatures up to +12°C are

recorded in the Molodezhnaya station¹¹ and can reach up to 20°C in the Ross Sea region during the austral summer.¹² Because microbial diversity is related to soil chemistry,¹³ that is, in turn, influenced by microclimatic conditions,¹⁴ dynamically changing permafrost conditions accompanying climate change will likely cause shifts in the cryosphere's microbial population.¹⁵

Antarctic soils record signatures of climate change as well as information on the glacial history of the MDVs.^{3,16-18} These hyperarid soils form through an interplay between cryogenic (fragmentation by glacial retreat and mechanical and chemical weathering) and microclimatic processes (precipitation, katabatic winds, and ice sublimation). However, despite the impressive microbial diversity within a range of cryospheric habitats,^{1,19,20} the role of psychrotolerant (cold-tolerant)

bacteria in silicate weathering has not been deeply investigated, except in organic-rich and relatively humid soils of eastern Antarctica.¹¹

All polar glacial settings exert extreme environmental conditions such as high ultraviolet (UV) light fluxes, extreme cold, nutrient deficiency, high salinity, and aridity.²¹ As one moves from the coastal regions to inland, the microclimatic zones gradually become hyperarid and colder from mixed xerous in the MDVs (50–200 mm/year precipitation) to ultrixerous (0–50 mm/year precipitation) zones in high-altitude mountain ranges,^{22,23} thus potentially decreasing biological diversity and curtailing microbial activity. However, polyextremophilic microbes have evolved multiple survival strategies such as pigment, exopolymeric substance (EPS), cold-adaptive enzymes, and osmoprotectant production that allow them to cope with their extreme environments.^{21,24,25} Moreover, microbial cells can persist within ice (e.g.,^{26,27}) and permafrost up to a few million years and may still be capable of sustaining basic metabolic activities.^{28–30} Therefore, we hypothesize that as permafrost warms, microbial communities may enhance silicate weathering in polar environments, even in xerous and ultrixerous settings.

Previous studies of Antarctic ephemeral meltwater streams revealed that solute fluxes indicate active chemical weathering of drift sediments, even under kinetically limited extremely cold conditions and short periods of liquid water availability.^{31–33} Higher-than-expected nutrient concentrations of these streams also show evidence of additional microbial silicate weathering contributing to chemical weathering pathways along these streams.³⁴ In addition, biotically promoted weathering in arid settings of the MDV such as rock crevices and pores occurs as a result of micro-acidic conditions produced within the EPS layer and mechanical weathering via EPS expansion along with lichen and filament placement.^{35–40} MDV soils also have C and N isotopic signatures, indicative of partial soil formation by microbial life within endolithic environments.⁴¹ Furthermore, cyanobacteria may have formed primordial soils of early Earth, and prospective extraterrestrial soil formation processes on Mars and other bodies may also be tied to biow weathering by polyextremophiles.^{30,41} Traces of such biological surface alteration can be used as inorganic biosignatures, which are defined as the chemical, morphological, and mineralogical (biomineral) biproducts of microbe-mineral interactions.^{42,43}

Considering the compelling evidence of chemical and potentially biological weathering from previous studies in Antarctica (e.g.,^{35,41}) and the role of microbes in accelerating silicate weathering (e.g.,^{44–47}), we hypothesize that cyanobacterial mats in polar environments have the potential to enhance chemical weathering rates via both elevated pH in the solution and locally generated micro-acidic regions within their EPS on the grains via cell-surface attachment. Therefore, we predict that the cyanobacterial mats could cause significant changes in the aquatic chemistry and detectable mineralogical changes in sediments and/or proto soils within glaciated planetary settings. Here we report the results from comparative biotic and abiotic silicate weathering experiments at 12°C on mixed felsic-mafic, fine-grained (<63 µm), pre-weathered proglacial sediments of the Onyx River

(Wright Valley [WV]) that derive from MDV drifts. Although the focus is on Antarctic biow weathering and the relationship to biogeochemical processes in the permafrost, we include a separate set of experiments on basaltic glacio-volcanic outwash deposits from Iceland to compare biow weathering effects on fresh mafic sources in Arctic regions and predict potential biow weathering processes on other icy planets such as Mars.

2 | METHODS

2.1 | Starting material: source, preparation, and characterization

To quantify the weathering rates of silicate minerals derived from different bedrock compositions in glacial regions, we used glacial meltwater sediments collected from Antarctica (mixed felsic-mafic source materials) and Iceland (uniform mafic source), representing glacial drift deposits. Sediments were collected by G.S. Soreghan, M.E. Elwood Madden, and previous researchers from slackwater regions of marginal channel bars^{32,33,48,49} and stored at –21°C until further analysis. We obtained the Antarctic sediments from the Onyx River ($n = 3$; 77° 27.003' S, 162° 29.858' E; 77° 27.318' S, 162° 28.581' E; 77° 27.787' S, 162° 26.567' E, collected in January 2010), a MDV meltwater stream emanating from cold-based Wright Lower Glacier and Clark Glacier in WV. The Onyx River drains from Lake Brownworth and passes through pre-Last Glacial Maximum glacial sediments derived from the Ferrar Dolerite, and plutons composed of diorite, granite, granodiorite, and quartz monazite flowing into Lake Vanda.^{18,33} We additionally collected various drift deposits, meltwater stream sediments, and soil samples from both Wright and Taylor Valleys to compare their microtexture and weathering features with the ones to be produced in experimental samples. We obtained the basaltic Iceland sediments from the modern glacial outwash stream of the Eyjafjallajökull volcano ($n = 3$; 63° 40.858' N, 19° 38.032' W; 63° 40.976' N, 19° 38.168' W; 63° 40.178' N, 19° 37.504' W; collected in May 2017) to investigate abiotic and biotic weathering of fresh mafic glacio-volcanic deposits, similar to those expected on Mars.⁵⁰

Before any sample was processed, we sputter-coated a subsample of the Antarctic sediments with Au/Pb and imaged them using scanning electron microscopy (SEM) with energy dispersive X-ray spectroscopy (EDS). This imaging enabled the observation of the natural state of the samples and examination of any preexisting weathering features and biofilms (Figure 1).

We merged the three Onyx River sediments together into one batch and three Eyjafjallajökull outwash sediments into another and then wet sieved the two samples through a <63-µm mesh to obtain the “glacial-fine”⁵¹ mud-sized fraction. We focus on the fine-grained components of the sediments because these have the most abundant surface area for alteration, allowing us to observe solute fluxes in short-term weathering reactors. Although weathering also occurs on larger grains, it proceeds more slowly and does not generate

FIGURE 1 SEM (scanning electron microscopy) images of untreated Antarctic drift (b: Ross Sea Drift, TV [Taylor Valley]), sediment (a, e, f: Delta Stream, TV; d: Clark Glacier Stream, WV [Wright Valley]), and soil (c: Upper Onyx River, WV) samples. Numbers indicate EDS (energy dispersive X-ray spectroscopy) measurement locations (Table S6). (a) Side-by-side comparison of a biofilm-covered (arrow) and uncolonized smooth grain shows that biofilms effectively disintegrate the sediments. (b) Incongruent dissolution pits formed via abiotic weathering and secondary blade-like potential Ca-carbonates (EDS 1) and spherical Fe-bearing carbonates (EDS 2) are observed. (c) Exfoliation (flaking) of the mineral surface (arrows). (d) Exfoliation features are generally associated with biofilms (arrows). (e) EPS (exopolymeric substance) covering mineral surfaces leave large grooves on mineral surfaces via etching (arrows). (f) Close-up of the etched grooves in Figure 1e (white box) shows nanophase spherical Fe precipitates (putative inorganic biosignatures) nucleating on and within the biofilm layer

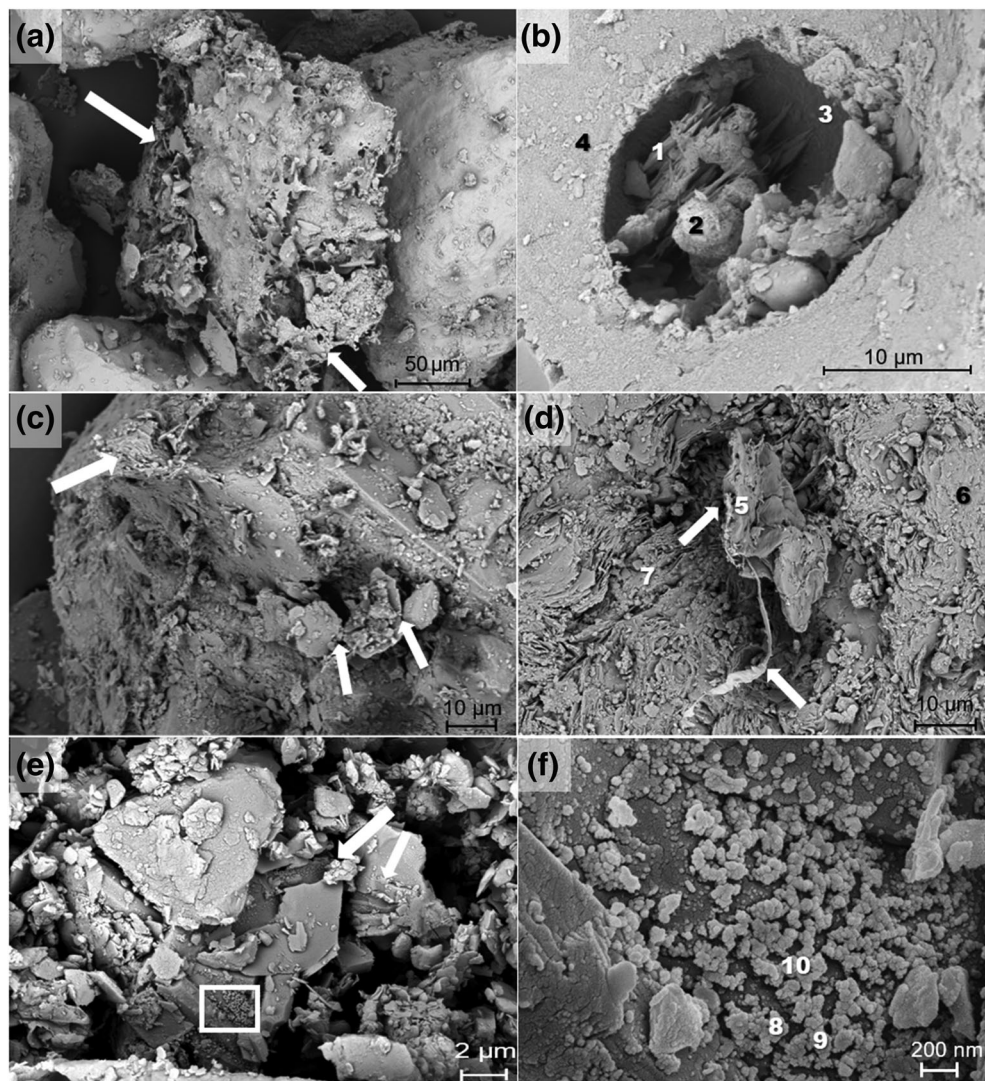


TABLE 1 Physical characteristics of Antarctic and Icelandic sediments

Location	BET (m ² /g)	Clay (<4 μm) grain size (%)	Silt (4–63 μm) grain size (%)
Antarctica	8.2	3.8	96.2
Iceland	11.5	2	98

Note. BET, Brunauer–Emmett–Teller.

TABLE 2 Chemical and mineralogical characteristics of Antarctic and Icelandic sediments

Location	SiO ₂ (%)	Al ₂ O ₃ (%)	P ₂ O ₅ (%)	Fe ₂ O ₃ (%)	MnO (%)	Mafic minerals (%)	Quartz + K-spar (%)	Plagioclase (%)	Clay minerals (%)	Amorphous phases (%)
Antarctica	56.4	15	0.3	8.6	0.1	12.2	16.2	28.8	37.6	3.2
Iceland	52.9	15.6	0.5	11.8	0.2	25.9	0	38.7	0	31.6

significant weathering fluxes.^{51,52} We treated the samples with glacial acetic acid (24 hours) and hydrogen peroxide (3 days) to remove secondary carbonate and organic remnants (cell, biofilm, and other organic matter) and/or sulfide fractions, respectively.^{32,42} These treatments isolated the silicate fraction, thus simplifying the design and allowing us to focus on the aqueous and mineralogical changes resulting solely from silicate weathering and microbial activity.

Following the chemical treatments, we determined the clay and silt fractions within these glacial fines (Table 1) using a Malvern Mastersizer 3000 laser particle size analyzer, after treatment with sodium hexametaphosphate as a dispersant.⁵³ We quantified the specific surface area of the glacial fines (Table 1) using the Brunauer–Emmett–Teller (BET) nitrogen adsorption method, with a Quantachrome Nova 2000e gas adsorption analyzer,^{54,55} and determined

the mineralogy of the glacial fines with X-ray powder diffraction (XRD) using a Rigaku Ultima IV with a Cu radiation source and graphite monochromator (Figures S2 and S3). We mounted the sediments in standard glass sample holders and employed the Bragg–Brentano method (2–70° 2θ angle interval). Analyses were performed with 0.02° step size and 2-second counting time, using fixed slits. We determined the mineral composition quantitatively (Table 2) with MDI Jade software using the Reitveld refinement method^{56,57} in combination with ClaySIM software using the RockJock method.⁵⁸ Finally, we sent our samples to ALS Labs (ALS USA Inc., Reno, NV, USA) for whole rock geochemistry (Inductively Coupled Plasma Mass Spectrometry (ICP-MS), Li borate fusion method) and trace element and base metal geochemistry (Inductively Coupled Plasma Atomic Emission Spectroscopy (ICP-AES), acid-digestion methods).

2.2 | Culture growth and experimental design

We purchased the polyextremophilic culture, *Leptolyngbya glacialis* (ULC073), from Belgian Coordinated Collections of Microorganisms. This culture is non-axenic (also contains some heterotrophic cells) due to the difficulties in isolating filamentous cyanobacteria.^{59,60} We grew the culture at 12°C in 1× BG11 freshwater medium (Sigma-Aldrich, St. Louis, MO, USA, catalog #C3061, adjusted pH 7 with 1 M KOH) in a rotary shaking incubator (Inova 42R with cyanobacterial growth lamp) at 60 rpm for 3 weeks, providing an 8-hour dark/16-hour light cycle (Figure S1b), representing optimal conditions for the strain. Then, we inoculated ~25 mg of wet cells into 50-ml sterile glass Erlenmeyer flasks containing 25-ml sterile 0.1× BG11 and 0.25 g of UV-sterilized muds, in triplicates to set up biological weathering experiments. We set up abiotic controls containing UV-sterilized mud and 25-ml 0.1× BG11. Each separate batch reactor experiment lasted 0, 1–2, 3, or 4 weeks, representing varying durations of the Antarctic melt season. In addition, we set up parallel culture growth controls

(without adding sediments) to monitor the pH and microbial growth in the absence of nutrient flux from weathering. We monitored the cyanobacterial growth in 0.1× BG11 medium for 6 weeks to obtain data points at all phases on its growth curve (lag, exponential, stationary, and death).

2.3 | Sampling and analyses during the experiments

We sampled individual batch reactors (in triplicate) of Icelandic biotic weathering experiments at week 0, 2, 3, and 4. Chlorophyll-a (Chl-a) measurements demonstrate that the culture showed considerable growth in the first week.⁴² Therefore, we added a week-1 sampling time point to the later Antarctic weathering experiments. During each sampling, we filtered supernatants through 0.2-μm syringe-tip filters to remove particulates and cells from the solution, and we periodically measured the pH of the filtrates. We sent separate aliquots of the filtrates (untreated) for ion chromatography and acidified (1 M HNO₃) aliquots of the filtrates for ICP-AES analyses (The Advanced Water Technology Center and J. Ranville Lab at the Colorado School of Mines, Golden, CO, USA) to monitor all released anions and cations. We also monitored the changing alkalinity via bicarbonate and carbonate ion measurements (flow injection method, OSU Soil Labs, Stillwater, OK, USA).

2.4 | Weathering rate calculations

Weathering rates were measured based on aqueous silica concentrations observed during both the abiotic and biotic weathering experiments. We calculated Si weathering rates by plotting aqueous Si concentrations (obtained by ICP-AES) normalized to BET surface area of sediments versus time elapsed (Figure 2) and then fitting the curve

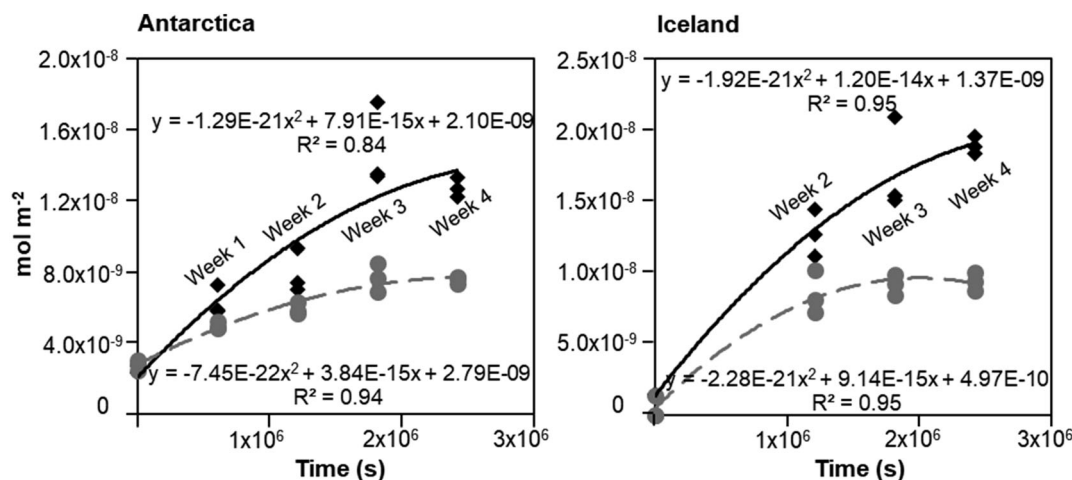


FIGURE 2 Antarctic and Icelandic silica release normalized to BET (Brunauer–Emmett–Teller) surface area (mol/m²). Solid black and dashed gray lines are biotic and abiotic weathering trend lines, respectively. Note the higher biotic weathering rates (diamonds) as compared to abiotic weathering rates (circles)

with a polynomial equation. We used the first derivative of the polynomial to determine the rate of biological and abiotic weathering.⁶¹

2.5 | Microbial growth monitoring

We monitored cyanobacterial growth within both the biotic weathering experiments and culture growth controls via Chl-a measurements on microbial mats. We harvested and weighed cell pellets weekly (centrifuged at 12,000g for 10 minutes in preweighed tubes). We extracted Chl-a in 90% methanol at 25°C in the dark and measured the absorbance values of the extract at 663 nm using UV/Vis spectrophotometry (Genesys 6, Thermo Scientific, Waltham, MA, USA). We also measured the absorbance values at 750 nm to correct for interreference and calculated Chl-a concentrations using Equation 1.^{62–64}

$$\text{Chl-a} (\mu\text{g}/\mu\text{l}) = \text{Absorbance} (663-750\text{nm}) \times 12.7 \quad (1)$$

We also performed the same extractions and spectrophotometric measurements on the sediments of the abiotic experiments to account for remnant Chl-a (if any) or other green pigments coming from the field. Then we corrected the absorbance values of biotic experiments by subtracting the absorbance values of abiotic experiments. This correction allowed us to ensure that our results represent only cyanobacterial growth.

2.6 | Imaging microbial mats, weathering features, and secondary mineral formation

To preserve the biofilm structure for SEM imaging, we fixed sediment–microbe aggregates on pre-sputter-coated glass slides immediately on harvesting using a mixture of 2.5% glutaraldehyde, 50mM lysine, and 0.1 M HEPES buffer (pH 7). Then we successively applied a secondary fixation (1% OsO₄ in 0.1 M HEPES), EtOH dehydration (25%, 50%, 75%, 95%, and 100%), and finally chemical drying (HMDS:EtOH ratio 1:2, 1:1, and 2:1) protocols suggested for microbial biofilms.^{65,66} We sputter-coated with Au/Pd (10-nm coating) to create conductive specimens and then imaged biofilms, cells, and potential microbial weathering features (e.g., cell-shaped pits) using SEM. We also coupled EDS measurement with our imaging to determine elemental composition changes on the grains and characterized secondary precipitates, thus identifying and characterizing inorganic bio-signatures of surface alteration.⁴² We performed our SEM-EDS studies at the OU Samuel Roberts Noble Microscopy Laboratory, using Zeiss NEON 40 EsB field emission SEM with an Oxford Electron Backscattered Diffraction camera and INCA Energy 250 energy dispersive X-ray microanalysis system. We used a combination of secondary electron, backscattered diffraction, and InLens detectors alternating between 5 and 15 kV, depending on surface charging, organic matter content, and scale of the mineral or bacteria to image.

2.7 | Statistical analyses

To determine the significance of our results, we performed four multivariate statistical analyses^{67–69} on abiotic and biotic weathering experiments, separately for Antarctica and Iceland reactors, using GraphPad Prism 9.0.2 software. We performed PCA (principal component analysis⁶⁷) with principal components (PCs) with eigenvalues greater than 1.0 (Kaiser rule). Plots of PCs are grouped based on the presence of microbes (biotic or abiotic) and overlapped with loading vectors showing which water chemistry variables (solutes and pH) are driving the most significant differences. We also performed multiple unpaired *t*-tests using two-stage step-up Benjamini, Krieger, and Yekutieli procedure controlling the false discovery rate,⁷⁰ comparing the water chemistry at each time point between abiotic and biotic experiments to identify the significant differences. Finally, we plotted *r* scores from Pearson's correlation matrix to prepare separate heat maps for Antarctica and Iceland experiments to determine which water chemistry changes are significantly correlated with each other in both biotic and abiotic reactors. High positive correlation is indicated by *r* scores between 0.5 and 1, increasing in degree with higher *r* scores, whereas high negative correlation between the two variables is indicated by *r* scores between –0.5 and –1. Finally, we supplemented these tests with two-way ANOVA (analyses of variance) coupled with Tukey's multiple comparisons⁶⁸ on our solute chemistry, using *p* < 0.05 threshold as an indication of significant microbial influence on silicate weathering. Here we also investigated the significance of pH and Chl-a increase between comparable biological weathering and culture growth experiment time points using two-way ANOVA coupled with Šídák's multiple comparisons.

3 | RESULTS

3.1 | Weathering features observed in the field

SEM imaging of the untreated field samples shows mechanical, biological, and abiotic weathering textures in Antarctic drift sediments and soils (Figure 1). Side-by-side comparisons of colonized and uncolonized samples (Figure 1a) illustrate that biofilm cover results in the disintegration of the grain surfaces, whereas uncolonized grains do not disintegrate. Chemical incongruent dissolution features were discernable as smooth-pitting and blade-like Ca-rich secondary precipitates, Fe-bearing carbonates, and potential Fe coatings on pit walls (Figure 1b; Table S6). Biofilms and filaments also contribute to mechanical and chemical weathering by separating the grains (Figure 1c,d), dissolving them (Figure 1e), and leaving nano-phase secondary precipitates (Figure 1f). Exfoliation structures observed (Figure 1c,d) may be artifacts of both mechanical disintegration by the microbial mats and weathering by acidic chemical solutions. SEM coupled with EDS measurements revealed that nano-phase potentially neo-formed precipitates are Fe-(oxy)hydroxide minerals on mafic grains impacted by biofilms (Figure 1f).

3.2 | Weathering experiments

3.2.1 | Characteristics of the treated starting material

Specific BET surface area values of the Antarctic and Icelandic sediments are 8.2 and 11.5 m²/g, respectively. The bulk SiO₂ and Al₂O₃ contents, as well as the grain size (silt/clay), are comparable (Tables 1 and 2). The primary difference between the Antarctic and Icelandic samples is their contrasting mineralogy. The Antarctic sample contains more felsic primary minerals and clay minerals (largely smectite and

illite), whereas the Iceland sample contains more mafic phases and amorphous materials (Table 2; Figures S2 and S3).

3.2.2 | Silica release rates

Silica release rates in all of the Antarctic mixed-source experiments were significantly slower than the silica release rates observed in the mafic Icelandic experiments, in both the biotic reactors and abiotic controls (Table 3; Figure 2). Within the mafic Icelandic sediments, we observed little difference between the bioweathering and abiotic

TABLE 3 BET-normalized comparative Si release rates (mol/m²s)

Replicate	Antarctica			Iceland		
	Biotic	Abiotic	Biotic/abiotic	Biotic	Abiotic	Biotic/abiotic
1	7.0×10^{-15}	4.0×10^{-15}	1.8	1.0×10^{-14}	9.0×10^{-15}	1.1
2	1.0×10^{-14}	3.0×10^{-15}	3.3	9.0×10^{-15}	1.0×10^{-14}	0.9
3	9.0×10^{-15}	2.0×10^{-15}	4.5	1.0×10^{-14}	9.0×10^{-15}	1.1
Average	8.7×10^{-15}	3.0×10^{-15}	3.2	9.7×10^{-15}	9.0×10^{-15}	1.0
Standard deviation	1.3×10^{-15}	8.2×10^{-16}	1.1	4.7×10^{-16}	8.2×10^{-16}	0.1

Note. BET, Brunauer–Emmett–Teller.

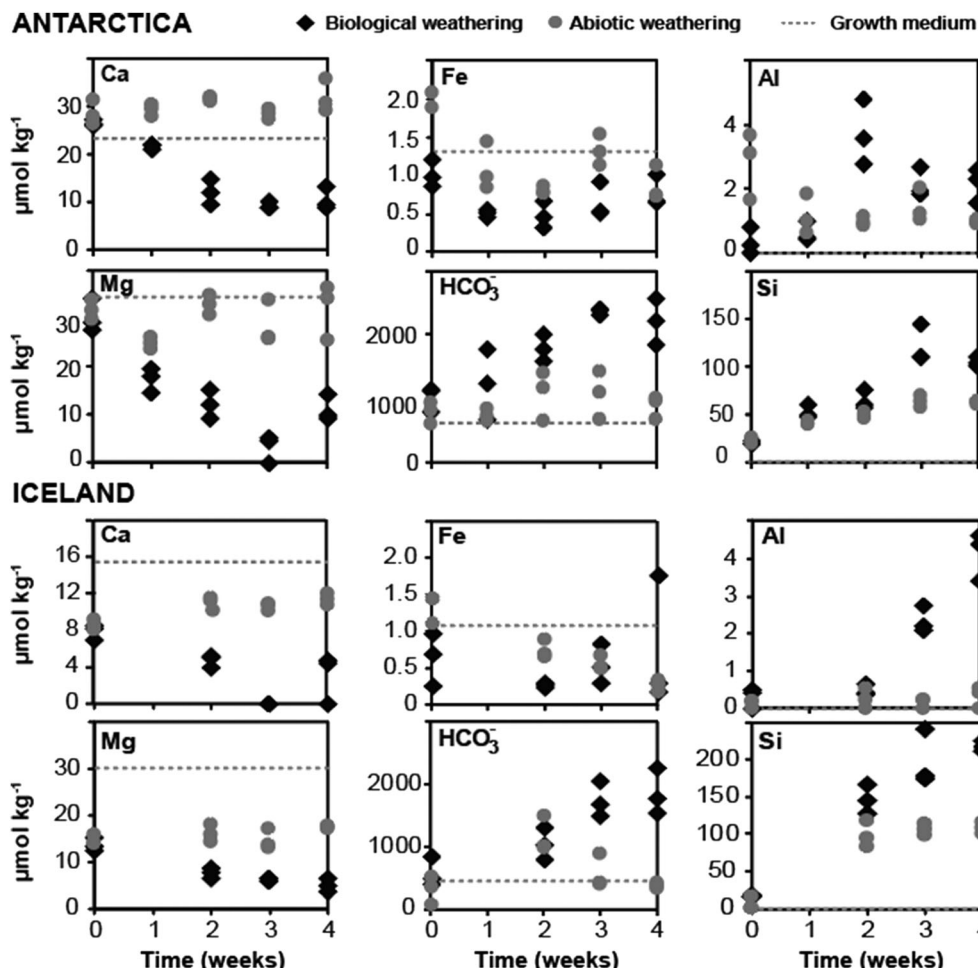


FIGURE 3 Changes in solute chemistry during Antarctic and Icelandic biotic (diamonds) and abiotic (circles) experiments. Dotted lines mark initial concentrations in the growth medium. Note the significant biotic intake of bioessential nutrients (Ca, Mg, Fe), whereas HCO₃⁻, Al, and Si increase due to silicate weathering

weathering rates. However, in the more felsic, mixed-source Antarctic sediments, the bioweathering rates were up to three times faster than the abiotic controls (Table 3; Figure 2).

3.2.3 | Aqueous chemistry and chlorophyll production

We observed increasing Si, Al, and HCO_3^- concentrations in both biotic and abiotic reactors for the Antarctic and Icelandic silicate weathering experiments; however, the final concentrations of Si, Al, and HCO_3^- were significantly higher in the presence of microbial life (Figure 3; Table S1). Nutrients important for biota (Ca, Fe, Mg, Mn, P, NO_3^- , SO_4^{2-}) decreased significantly in all biotic reactors (Figures 3 and 4; Table S1). These solutes changed only slightly or remained constant in all abiotic reactors (Figures 3 and 4; Table S1). This trend is also observed in the Fe plots, where Fe was nearly

depleted in the solution by the end of week 2 in the biological experiments and then increased, whereas Fe decreased throughout the abiotic experiments.

Solution pH increased from 6.5 through 7 in abiotic weathering experiments and up to 8 in biological weathering experiments and culture growth controls (Figure 5; Table S2). pH increases in the biotic reactors were accompanied by increasing Chl-a (Chl-a) pigmentation (Figure 5; Table 2). Differences in Chl-a between each of the three biotic replicates likely result from sampling both microbial cells and biofilm within the microbial mat. Chl-a concentrations depend on the amount of the active cyanobacterial cells; however, the weight of the biofilm (e.g., EPS components) and the actual cells cannot be differentiated. For example, the highest Chl-a concentrations within the three replicates should correspond to the highest weight of cyanobacterial cell density within the sampled microbial mat, even though the total microbial mat (cell + biofilm) weights are almost the same.

3.2.4 | Statistical analyses

PCA analyses (Figure S4) revealed that pH, Si, HCO_3^- , Al, and Fe solute concentrations resulted in the most significant differences in both Iceland and Antarctic experiments, where pH, Si, HCO_3^- , and Al correlate strongly with biotic pathways, whereas Fe solute concentrations show the most difference in abiotic experiments. Significant differences in water chemistry between biotic and abiotic weathering experiments occur starting with the first and second weeks of the experiments but accentuated in the third and fourth weeks. As expected, no significant differences occurred between week 0 samples. The results of the t-tests (Table S3) are in agreement with all PCA results. t-Test analyses also show that Ca, Mn, Al, Mg, P, SO_4^{2-} , and NO_3^- are significantly different between biotic and abiotic experiments due to significant decreases in aqueous concentrations in biotic experiments (Figures 3 and 4; Table S1). Pairwise comparisons indicate that all investigated water chemistry variables, except Fe, are significantly different between biotic and abiotic experiments at the end of 4 weeks. Two-way ANOVA pairwise comparisons of biotic and abiotic solute chemistry (Table S4) are in agreement with PCA and t-test results. In addition, pairwise comparisons of biotic and culture growth comparisons of pH and Chl-a results indicate no significant differences between comparable time points, besides higher mean Chl-a in biotic at weeks 3 and 4 of Antarctic and Icelandic experiments, respectively (Table S5). Finally, Pearson's correlation tests (Figure 6) of both biotic and abiotic experiments showed high positive correlation between Fe-P and Ca-Mg. These results are in strong agreement with the PCA analyses; Si is highly correlated with pH, HCO_3^- , and Chl-a in all biotic reactors, with the addition of high correlation to Al in Iceland biotic experiments, indicating a high positive correlation of silicate weathering to photosynthesis. In addition, microbially important nutrients (Ca, Mg, Mn, P, SO_4^{2-} , and NO_3^-) are highly positively correlated with one another in both Antarctic and Icelandic biotic experiments, whereas similar trends and/or strong correlations are not observed in abiotic experiments. Overall, the

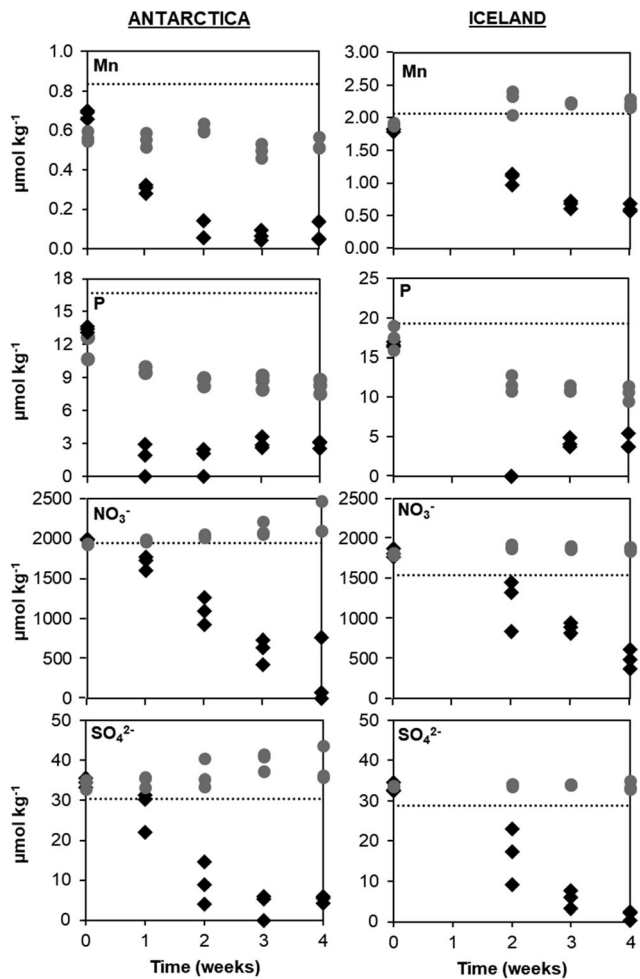


FIGURE 4 Changes in Mn, P, NO_3^- , and SO_4^{2-} concentrations during Antarctica and Iceland biotic (diamonds) and abiotic (circles) weathering experiments. Mn, P, and NO_3^- are consumed by *Leptolyngbya glacialis* as they are essential for the photosystems. SO_4^{2-} depletion in the biological experiments is likely due to microbial use

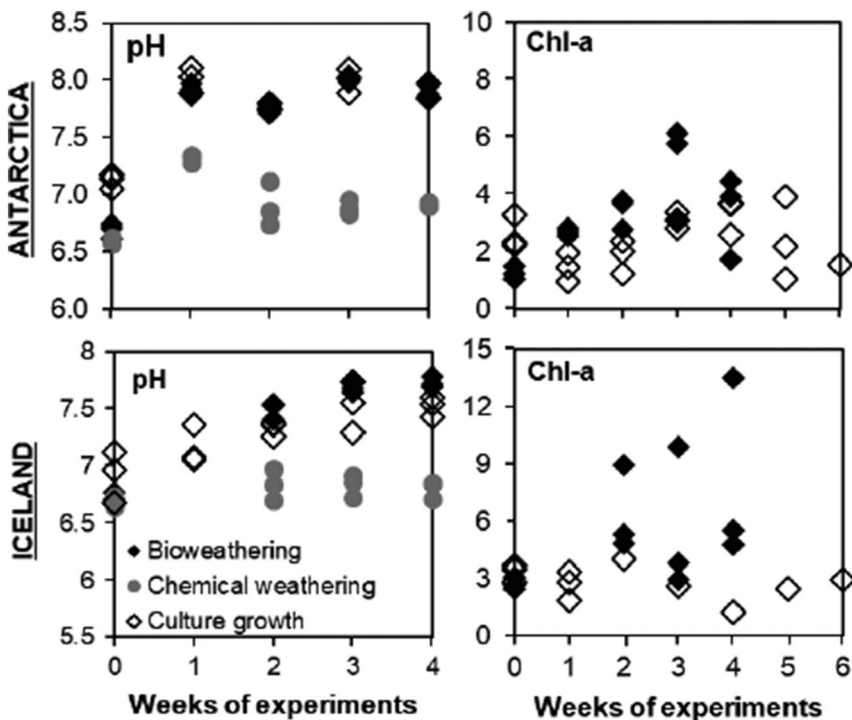


FIGURE 5 Changes in pH and chlorophyll-a (Chl-a; $\mu\text{g}/\text{ml}$) during Antarctic and Icelandic biotic (solid diamonds) and abiotic (circles) experiments. Hollow diamonds indicate culture growth experiments. Note the increase in pH with Chl-a in biowathering and culture growth experiments due to photosynthesis, as opposed to nearly constant abiotic pH

combined statistical results are in agreement pointing to significant differences in water chemistry driven by *L. glacialis*.

3.2.5 | SEM observations

Although we did not observe any discernable textural changes in the abiotic experiments (Figure 7a), we did observe a few chemically weathered surfaces (Figure 7b), where weathering starts from a corner and regularly moves across the grain surface, leaving a very shallow pitted surface (Figure 7c) that is different from its biogenic counterparts (e.g., Figure 7f). We observed several features indicating biological weathering in the SEM images collected from Icelandic biotic experiments (Figure 7d–f). For example, the cyanobacteria physically trapped grains within a mesh of filaments and were bound to the sediments with their biofilms (Figure 7d). Biofilm and cell attachment also dissolved the grains, leaving filament or coccus-shaped etch pits (Figures 7e,f and 8a) on grain surfaces, and potentially aided the formation of secondary Fe-oxy(hydroxide) and flakey clay precipitates on mineral and cell surfaces (Figures 7e and 8b,c). Botryoidal etch pits resembling coccus colonies (Figure 7f) were also observed and may potentially reflect heterotrophic communities (potentially *Deinococcus* sp. in MDV soils⁷¹) that came with the microbial mat.

4 | ENHANCED WEATHERING BY MICROBES IN SEDIMENTS

These results show that *L. glacialis* enhance Si release rates up to threefold relative to abiotic weathering (Table 3; Figure 2) in the

mixed-source Onyx River sediments, comparable to Si release rates at 25°C from *Leptolyngbya* strains collected in temperate glacial environments.⁴⁵ Increased weathering rates in biotic reactors relative to abiotic controls likely relate to acidic microenvironments developed beneath microbial biofilms (e.g.,⁷²), forming the cell-shaped etch pits observed by SEM imaging (Figure 7). Organic acids produced within the EPS also likely facilitated the extremely high Al release observed (Figure 3; Table S1).⁴⁰ However, the overall pH increases in biotic experiments (up to ~8) track closely with the pH observed in the culture growth controls, accompanied by increasing Chl-a, suggesting that the overall pH is largely controlled by photosynthesis (Figures 5 and 6; Table S5). This overall increase in pH in the biowathering experiments likely contributed to enhanced Si release.⁴⁵ Chl-a pigmentation in the microbial mats peaked at weeks 2–3 and was replaced with carotenoid pigments likely as a result of prolonged exposure to UV radiation (Figure S1d and S1e) and NO_3^- depletion⁷³ (Figure 4). Decreasing Chl-a concentrations after weeks 2–3 also suggest that *L. glacialis* reached the stationary phase of their life cycle; solute concentrations also either stay constant or change more slowly (observed by relatively gentle slopes, Figures 3 and 4) around the same time, further relating solute release rates to microbial activity.

We observed faster weathering rates in both the biotic and abiotic mafic Icelandic weathering experiments compared to the mixed-lithology Antarctic experiments (Table 3), likely attributable to differences in chemistry and mineralogy (Table 2; Figures S2 and S3). Icelandic muds contain higher concentrations of fresh reactive mafic minerals (olivine and pyroxene) and volcanic glass, whereas nearly 38% of the Antarctic muds contain clay minerals (Table 2), which are less reactive. Because chemical weathering of the mafic minerals proceeds faster than rates observed for felsic minerals or clays,^{74,61} sufficient nutrients may be abiotically delivered to the bacteria in the

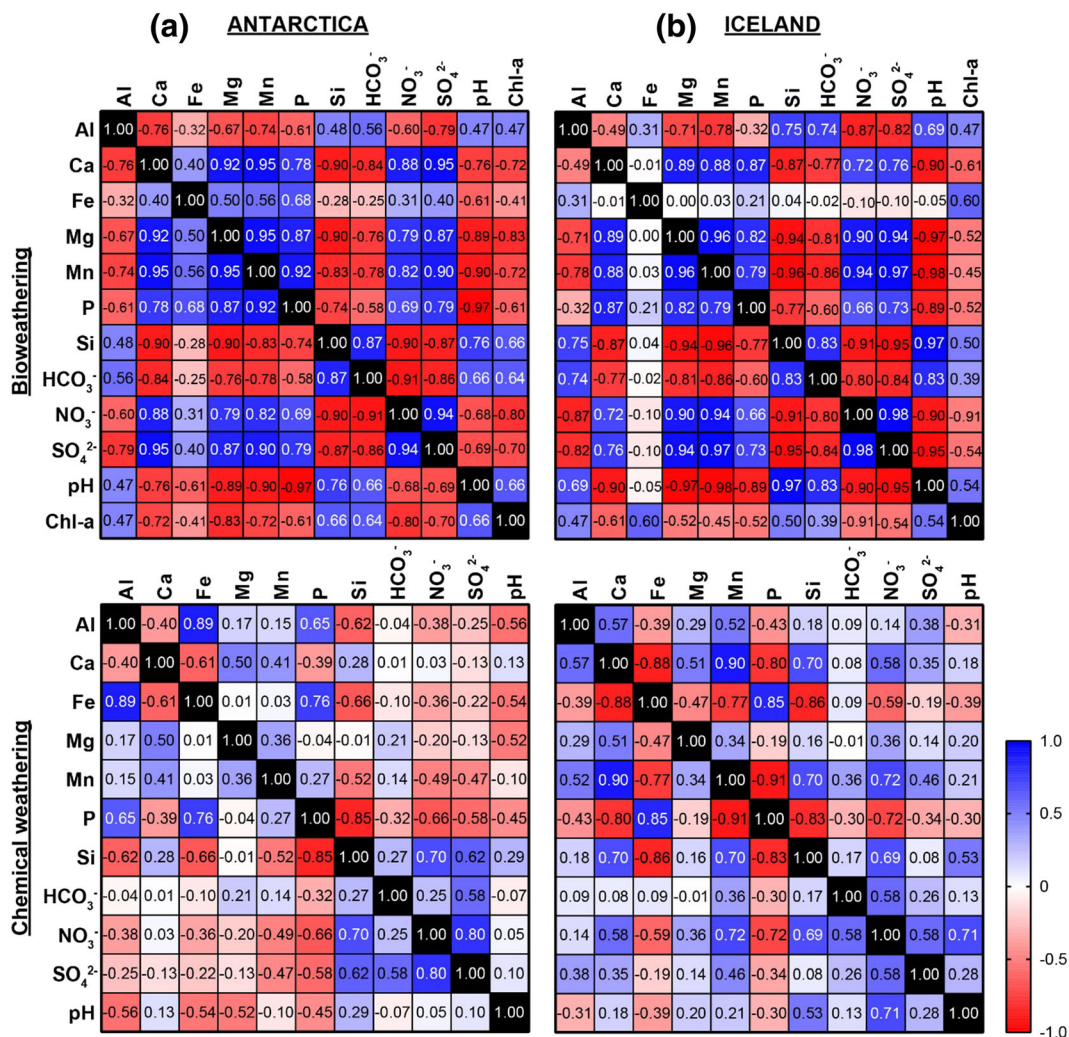


FIGURE 6 Pearson's correlation matrices of (a) Antarctic and (b) Icelandic bioweathering and abiotic weathering experiments. Numbers in the cells are calculated r scores, whereas color transitions from dark to light correspond to their graduation from higher to lower correlation. Red colors (negative values) indicate negative correlation, and blue colors (positive values) indicate positive correlation between the variables

mafic Iceland experiments, eliminating the need to scavenge nutrients through enhanced chemical weathering, leading to similar weathering rates observed in both the biotic and abiotic weathering experiments. In contrast, we posit that microbes stimulated chemical weathering in the Antarctic sediment experiments due to the lower nutrient release rates from less-reactive clays and felsic phases, resulting in nutrient-poor conditions that caused microbes to actively scavenge nutrients through biologically enhanced mineral dissolution reactions.

The Antarctic sediments have a complex weathering history dating from the Early-Mid Quaternary,⁷⁵ whereas Iceland sediments were freshly supplied by recent volcano-glaciogenic events.⁷⁶ Thus, the Antarctic sediments experienced prolonged “pre-weathering” before our experiments and thus were less reactive due to aging, in addition to differences in the source lithology. Wild et al.⁷⁷ found a nearly 10-fold increase in abiotic weathering rates from fresh labradorite and olivine minerals compared to artificially acid-aged samples in laboratory experiments.

Our water chemistry results show that nutrients essential for photosystems (i.e., Ca, Fe, Mn, Mg, and P)⁷⁸ decreased with increasing Chl-a production (Figures 3–5), consistent with potential secondary mineral precipitation and/or cellular intake by *L. glacialis*. SEM observations coupled with EDS measurements revealed potential neo-formed flakey secondary clay minerals (Figure 8c) and spherical nano-phase iron oxy/hydroxides (Figures 7e and 8b) associated with EPS and cell surfaces that are similar to the nano-phase minerals observed on biofilm-impacted grains in the field (Figure 1f). Previous studies suggest that such minerals in association with biofilms are potential biosignatures of microbial surface alteration.^{41,46,79,80} These secondary phases also consume cations from solution, resulting in lower aqueous concentrations, thus lowering the apparent weathering rates. In addition, survival mechanisms observed in polyextremophilic cultures (e.g., EPS and carotenoid production; Figure S1d and S1e) might consume added nutrients.

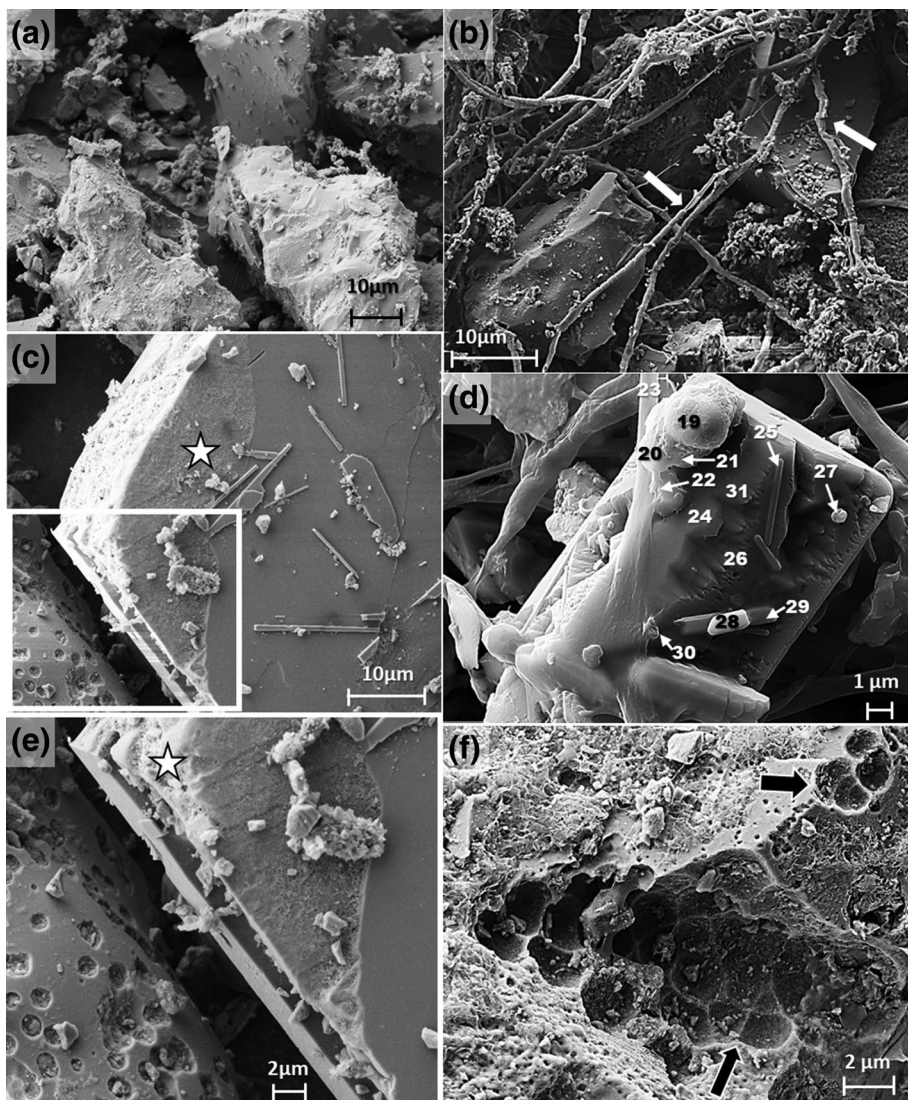


FIGURE 7 SEM (scanning electron microscopy) images from the fourth week of Icelandic abiotic and biological weathering experiments. Numbers indicate EDS (energy dispersive X-ray spectroscopy) measurement locations (Table S6). (a) Illustration of the overall case for abiotic experiments at a magnification of 1.17 k \times . Sediments in abiotic experiments illustrate mostly smooth surfaces. (b) *Leptolyngbya glacialis* filaments form a mesh trapping sediments and binding them with their EPS (exopolymeric substance) (arrows). (c) An etched surface (star) detected on a potential plagioclase grain. (d) A highly weathered Mg- and Fe-rich mineral (potentially olivine; EDS 24, 31) covered with biofilm (EDS 23) and colonized by bacteria (e.g., EDS 25), showing spherical secondary Fe-(hydr)oxide precipitation (EDS 20–21, 27, 30). Note that apatite minerals (EDS 28, 29) are detected on the surface, which might make the mineral favorable for colonization. (e) Close-up look at the boxed area in c. As expected, abiotic chemical weathering starts from the corner of the mineral (star) and creates a somewhat smoother surface as opposed to deep-pitted bioweathered minerals (e.g., F). Note that the lower left grain with pits is a vesicular basalt, not a weathered grain. (f) Etch pits (arrows) left by coccus (tetrad)-shaped colonies resembling B, indicating that other microbes in the mat assist weathering. Note that the mineral surface around the pits is flakey

Increasing Si dissolution (Figure 3) with increasing Chl-a production (Figure 5) indicates that weathering was enhanced by microbial activity in the biotic reactors. Overall, our results and statistical analyses indicate strong impacts of cold-tolerant cyanobacterial mats on silicate weathering, even in cold-arid conditions such as the Antarctic Dry Valleys. Our results also suggest that cyanobacteria likely play an important role in facilitating pedogenesis via silicate weathering in the MDV, as suggested by Mergelov et al.⁴¹

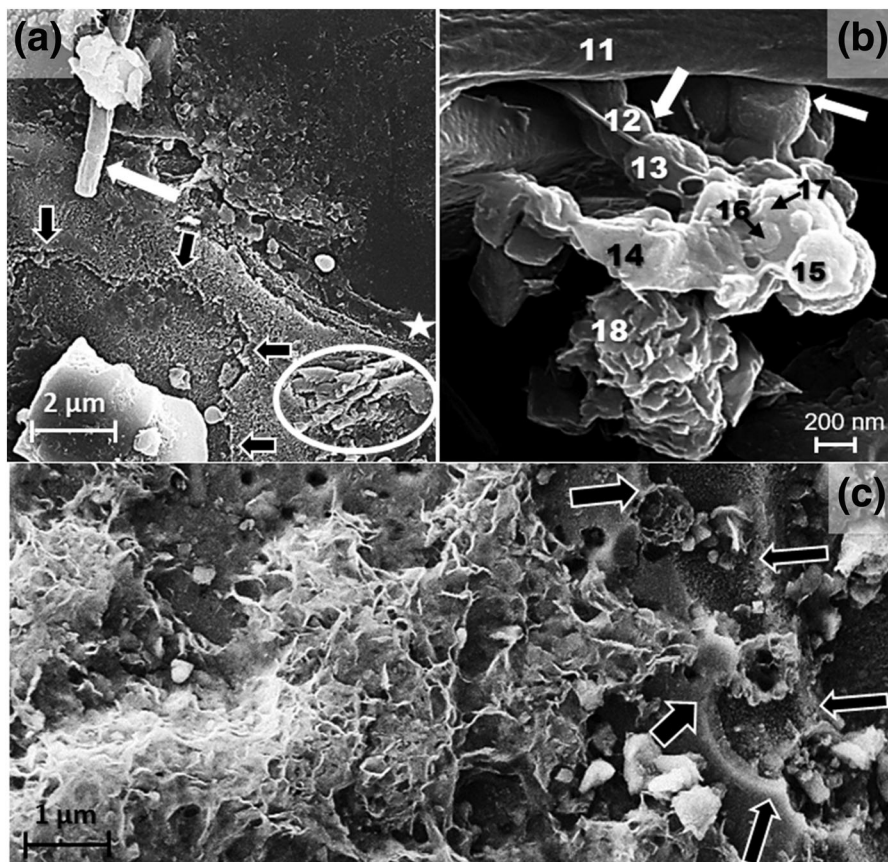
5 | IMPLICATIONS

5.1 | Carbonate production, chemical weathering, and nutrient cycling on Earth

Psychrotolerant polar cyanobacterial mats both enhance silicate weathering, releasing nutrients that promote primary production, and provide refugia for other organisms within their EPS. Cyanobacterial

FIGURE 8 SEM (scanning electron microscopy) images showing cyanobacteria filament-shaped etch pits, biominerals nucleating on cells, and flakey surface deposits in Icelandic bioweathering experiments. Numbers indicate EDS (energy dispersive X-ray spectroscopy) measurement locations (Table S6).

(a) *Leptolyngbya glacialis* (white arrow) and filament-shaped etch pit (star) on a mineral surface. Notice that the mineral surface displays other etching features associated with biofilm attachment (black arrows) and chemical dissolution (circle). (b) Secondary nano-phase Fe-(hydr)oxides (EDS 15–17) nucleating on coccus-shaped cell surfaces (white arrows, EDS 12–13) within the EPS layer (EDS 11) and a potential clay precipitate associated with biofilms (EDS 18). (c) Close-up of a region of flakey surfaces shown in Figure 7F. These honeycomb-like features are potentially neo-formed clays produced by bioweathering. Notice the stepwise etching associated with cells and biofilm traced by black arrows



mats also trap and bind mud-sized grains,⁸¹ creating an inorganic nutrition bank during prolonged nutrient-limited conditions.⁸² EPS excreted by psychrophilic cyanobacteria (Figure 7d,7e) likely helped some eukaryotes like microalgae (e.g.,⁸³) survive through cold climates and adapt to warmer environments by acting as a physical barrier.⁸⁴ Thus, psychrotolerant polyextremophilic cyanobacteria may have been crucial to sustain terrestrial life during paleoclimatic extremes, including Proterozoic glaciations such as Snowball Earth. Most of the Antarctic cyanobacteria, including those belonging to *Leptolyngbya* genus, are known for their cold tolerance and functionality across a wide range of temperatures (i.e., 4°C–23°C), making them good candidates for monitoring the effects of global warming⁸⁵ on soil processes such as weathering fluxes from silicate minerals.

Fresh, fine-grained sediment supplied by glacial milling and/or volcaniclastic processes fertilizes phototrophs,⁸⁶ stimulating further (bio)weathering and associated nutrient release and thus further enhancing phototroph activity in a positive-feedback cycle that greatly accelerates CO₂ drawdown. In our experiments, increased photosynthetic activity carried out by the cyanobacteria increased the pH due to CO₂ consumption, shifting the carbon speciation toward HCO₃[−],⁸⁷ thus resulting in four times higher HCO₃[−] concentrations compared to the abiotic weathering controls (Figure 3). Enhanced bicarbonate concentrations and cations released due to biological weathering of silicates could thus supersaturate oceans and promote the precipitation of carbonates, similar to those observed associated with Snowball Earth glaciations.⁸⁸

The results of our experiments provide insights into the effects of future warming of permafrost soils on the global C cycle. Although warming temperatures might cause the death of some strictly psychrophilic communities, growth rates of the psychrotolerant cyanobacteria will increase⁸⁵ in parallel with increasing nutrient fluxes that accompany higher chemical weathering rates. Nutrients resulting from combined abiotic and biotic chemical weathering pathways carried by meltwaters will fertilize the oceans³⁴ and periglacial soils. In addition, as microbial diversity is closely related with the chemistry of permafrosts,¹³ we posit that soil chemistry and mineralogy will change with intensifying weathering reactions and cause ecological shifts in soil microbial populations within glaciated settings. Based on our observations from untreated MDV sediments and our laboratory experiments, we posit that the Antarctic cyanobacterial mats have the potential to influence soil-forming processes and chemistry via enhanced silicate weathering and nutrient release, resulting in secondary mineral precipitation.

5.2 | Weathering and biosignatures on Mars

Microbe–mineral interactions leave biosignatures in the rock record and permafrost soils on Earth, providing clues to interpret similar chemical and mineralogical transformations within planetary soils. In our experiments we observed neo-formed clay and nano-phase Fe-(oxy)hydroxide precipitates (Figures 7e and 8b,c) similar to features

also observed in unprocessed field samples (see Figure 1f and^{41,46,79,80}). While secondary Fe and clay precipitates can also be precipitated solely by abiotic pathways, we did not observe them in our abiotic experiments. However, minerals observed on EPS and cell surfaces indicate the role of microbes in precipitating secondary phases through their biofilms. We observed these potential bio-minerals primarily on mafic minerals in unprocessed Antarctic drifts (Figure 1f) and throughout the bioweathered Icelandic sediments (Figures 7e and 8b,c).

Our findings suggest that cyanobacterial mats have the potential to produce putative biosignatures in mafic extraterrestrial terrains, thus providing biosignatures within the soils on other icy planets, especially Mars.^{42,55} Even though our experiments are not set up in Mars conditions, our felsic and mafic starting materials are sampled from sites (Antarctica and Iceland) considered to share climatic and mineralogic similarities to the Mars surface.^{42,50,55,57,89} Finding similar inorganic biosignatures, including spherical nano-phase Fe-(oxy)hydroxide minerals and clays associated with biofilm sheet-like etch surfaces and cell-shaped etch pits from mixed mafic-felsic terrains under SEM imaging (Figures 7e and 8b,c) in returned samples from the Perseverance Rover, might indicate the potential presence of past life on Mars.

6 | CONCLUSIONS

Our study demonstrates that psychrotolerant cyanobacterial mats significantly accelerate silicate weathering in mixed-source, pre-aged sediments by increasing the pH due to photosynthesis and EPS production, under warming polar temperature conditions. Even though the weathering rates are higher, in general, in mafic and volcanic glass-rich polythermal terrains in more temperate settings, chemical and biological weathering are almost of equal importance in terms of nutrient release as fresh mafic minerals can be easily weathered by abiotic pathways. In terms of the global C cycle, the biotic pathways accelerate atmospheric CO₂ withdrawal and bicarbonate production through weathering and shifting the saturation state toward carbonate via pH increase. As anthropogenic climate change (warming) continues, we posit cyanobacterial mats will contribute increasingly to significant changes in the permafrost in the MDV, altering the soil chemistry through enhancing fluxes of Si, Al, and HCO₃⁻, thus promoting the formation of clay and carbonate deposits. Such psychrotolerant polyextremophilic mats would also leave their biosignatures of surface alteration in the form of spherical nano-phase Fe-(oxy)hydroxide minerals on micron-scale biofilm sheet-like etch marks and cell-shaped pits on mafic minerals within mixed mafic-felsic planetary terrains. Therefore, the occurrence of such putative bio-minerals in future sample return missions would indicate microbial influences on geochemical cycling within planetary regoliths and thus the presence of past extraterrestrial life.

ACKNOWLEDGMENTS

We thank Kristin Marra, Brenda Hall, and Alison Stumpf for sample collection; Nina D.S. Webb for her assistance in sample processing;

Preston Larson for his help in SEM imaging; Andy E. Elwood Madden for his help in XRD data analysis; and Claire Curry for her help in statistical data analysis. We also thank Amy Callaghan, Boris Wavrick, Bradley S. Stevenson, Paul Lawson, and Anne Dunn for providing access to microbiology lab equipment and facilities. Finally, we thank the anonymous reviewers' comments that helped us improve the quality of our publication.

This project is funded by NSF grant number 1543344, "Quantifying Surface Area in Muds from the Antarctic Dry Valleys: Implications for Weathering in Glacial Systems."

CONFLICT OF INTEREST

The authors report no conflicts of interest.

DATA AVAILABILITY STATEMENT

The data that supports the findings of this study are available in the supplementary material of this article.

ORCID

Cansu Demirel-Floyd  <https://orcid.org/0000-0002-5329-6058>

Gerilyn S. Soreghan  <https://orcid.org/0000-0001-6925-5675>

Megan E. Elwood Madden  <https://orcid.org/0000-0002-6735-4554>

REFERENCES

1. Anesio AM, Laybourn-Parry J. Glaciers and ice sheets as a biome. *Trends Ecol Evol.* 2012;27(4):219-225. <https://doi.org/10.1016/j.tree.2011.09.012>
2. Bockheim JG. Antarctic Soils and Climate Change. In: Bockheim JG, ed. *The Soils of Antarctica*. Cham: Springer International Publishing; 2015a:305-314.
3. Bockheim JG (Ed). *The Soils of Antarctica*. Cham: Springer International Publishing; World Soils Book Series; 2015b.
4. Ugolini FC, Bockheim JG. Antarctic soils and soil formation in a changing environment: A Review. *Geoderma.* 2008;144(1-2):1-8. <https://doi.org/10.1016/j.geoderma.2007.10.005>
5. Nielsen UN, Wall DH, Adams BJ, et al. The ecology of pulse events: insights from an extreme climatic event in a polar desert ecosystem. *Ecosphere.* 2012;3(2):art17. <https://doi.org/10.1890/ES11-00325.1>
6. Fountain AG, Lyons WB, Burkins MB, et al. Physical Controls on Ecosystem, Antarctica. *BioScience.* 2015;49:961-971. <https://doi.org/10.1525/bisi.1999.49.12.961>
7. Levy JS, Fountain AG, Gooseff MN, Welch KA, Lyons WB. Water tracks and permafrost in Taylor Valley, Antarctica: Extensive and Shallow Groundwater Connectivity in a Cold Desert Ecosystem. *Bull Geol Soc Am.* 2011;123(11-12):2295-2311. <https://doi.org/10.1130/B30436.1>
8. Guglielmin M, Cannone N. A permafrost warming in a cooling Antarctica? *Clim Change.* 2012;111(2):177-195. <https://doi.org/10.1007/s10584-011-0137-2>
9. Guglielmin M, Fratte MD, Cannone N. Permafrost warming and vegetation changes in continental Antarctica. *Environ Res Lett.* 2014;9(4):045001. <https://doi.org/10.1088/1748-9326/9/4/045001>
10. Bockheim J, Vieira G, Ramos M, et al. Climate warming and permafrost dynamics in the Antarctic Peninsula region. *Global Planet Change.* 2013;100:215-223. <https://doi.org/10.1016/j.gloplacha.2012.10.018>
11. Dolgikh AV, Mergelov NS, Abramov AA, Lupachev AV, Goryachkin SV. Soils of Enderby Land. In: Bockheim JG, ed. *The Soils of Antarctica*. Cham: Springer International Publishing; 2015:45-63.

12. Balks MR, Paetzold RONF, Kimble JM, Aislabie J, And Campbell IB. Effects of hydrocarbon spills on the temperature and moisture regimes of Cryosols in the Ross Sea region. *Antarct Sci.* 2002;14(4): 319-326. <https://doi.org/10.1017/S0954102002000135>

13. Aislabie JM, Jordan S, Barker GM. Relation between soil classification and bacterial diversity in soils of the Ross Sea region, Antarctica. *Geoderma.* 2008;144(1-2):9-20. <https://doi.org/10.1016/j.geoderma.2007.10.006>

14. Campbell IB, Claridge GGC. Permafrost Properties, Patterns and Processes in the Transantarctic Mountains Region. *Permafrost Periglac Process.* 2006;17:215-232. <https://doi.org/10.1002/ppp>

15. Yergeau E, Bokhorst S, Kang S, et al. Shifts in soil microorganisms in response to warming are consistent across a range of Antarctic environments. *ISME J.* 2012;6(3):692-702. <https://doi.org/10.1038/ismej.2011.124>

16. Bockheim JG. Functional diversity of soils along environmental gradients in the Ross Sea region, Antarctica. *Geoderma.* 2008; 144(1-2):32-42. <https://doi.org/10.1016/j.geoderma.2007.10.014>

17. Cannone N, Guglielmin M, Malfasi F, Hubberten HW, Wagner D. Rapid soil and vegetation changes at regional scale in continental Antarctica. *Geoderma.* 2021;394:115017. <https://doi.org/10.1016/j.geoderma.2021.115017>

18. Hall BL, Denton GH. Surficial geology and geomorphology of eastern and central Wright Valley, Antarctica. *Geomorphology.* 2005;64(1-2): 25-65. <https://doi.org/10.1016/j.geomorph.2004.05.002>

19. Cary SC, McDonald IR, Barrett JE, Cowan DA. On the rocks: The Microbiology of Antarctic Dry Valley Soils. *Nat Rev Microbiol.* 2010; 8(2):129-138. <https://doi.org/10.1038/nrmicro2281>

20. Cowan DA, Khan N, Pointing SB, Cary SC. Diverse hypolithic refuge communities in the McMurdo Dry Valleys. *Antarct Sci.* 2010;22(6): 714-720. <https://doi.org/10.1017/S0954102010000507>

21. Seckbach J, Rappelotto PH. Polyextremophiles. In: Wagner D, Bakermans C, eds. DeGruyter; 2015.

22. Bockheim JG. Global change and soil formation in the Antarctic region. In Post-Sem Proc 1st Int Conf Cryopedol, Russian Academy of Science, 1993, p. 132-140.

23. Bockheim JG, McLeod M. *Soils of Central Victoria Land, the McMurdo Dry Valleys;* 2015:117-148.

24. Edwards HGM, de Oliveira LFC, Cockell CS, Ellis-Evans JC, Wynn-Williams DD. Raman spectroscopy of senescent snow algae: Pigmentation Changes in an Antarctic Cold Desert Extremophile. *Int J Astrobiol.* 2004;3(2):125-129. <https://doi.org/10.1017/S1473550404002034>

25. Margesin R, Miteva V. Diversity and ecology of psychrophilic microorganisms. *Res Microbiol.* 2011;162(3):346-361. <https://doi.org/10.1016/j.resmic.2010.12.004>

26. Karl DM, Bird DF, Björkman K, Houlihan T, Shackelford R, Tupas L. Microorganisms in the accredit ice of Lake Vostok, Antarctica. *Science.* 1999;286(5447):2144-2147. <https://doi.org/10.1126/science.286.5447.2144>

27. Raymond JA, Christner BC, Schuster SC. A bacterial ice-binding protein from the Vostok ice core. *Extremophiles.* 2008;12(5):713-717. <https://doi.org/10.1007/s00792-008-0178-2>

28. Bidle KD, Lee SH, Marchant DR, Falkowski PG. Fossil genes and microbes in the oldest ice on Earth. *Proc Natl Acad Sci U S A.* 2007; 104(33):13455-13460. <https://doi.org/10.1073/pnas.0702196104>

29. Gilichinsky DA, Wilson GS, Friedmann EI, et al. Microbial populations in Antarctic permafrost: Biodiversity, Stage, Age, and Implication for Astrobiology. *Astrobiology.* 2007;7(2):275-311. <https://doi.org/10.1089/ast.2006.0012>

30. Rivkina E, Abramov A, Spirina E, et al. Earth's perennially frozen environments as a model of cryogenic planet ecosystems. *Permafrost Periglac Process.* 2018;29(4):246-256. <https://doi.org/10.1002/ppp.1987>

31. Gooseff MN, McKnight DM, Lyons WB, Blum AE. Weathering reactions and hyporheic exchange controls on stream water chemistry in a glacial meltwater stream in the McMurdo Dry Valleys. *Water Resour Res.* 2002;38(12):15-1-15-17. <https://doi.org/10.1029/2001WR000834>

32. Marra KR, Elwood Madden ME, Soreghan GS, Hall BL. Chemical weathering trends in fine-grained ephemeral stream sediments of the McMurdo Dry Valleys, Antarctica. *Geomorphology.* 2017;281:13-30. <https://doi.org/10.1016/j.geomorph.2016.12.016>

33. Stumpf AR, Elwood Madden ME, Soreghan GS, Hall BL, Keiser LJ, Marra KR. Glacier meltwater stream chemistry in Wright and Taylor Valleys, Antarctica: Significant Roles of Drift, Dust and Biological Processes in Chemical Weathering in a Polar Climate. *Chem Geol.* 2012; 322-323:79-90. <https://doi.org/10.1016/j.chemgeo.2012.06.009>

34. Lyons WB, Dailey KR, Welch KA, Deuerling KM, Welch SA, McKnight DM. Antarctic streams as a potential source of iron for the Southern Ocean. *Geology.* 2015;43(11):1003-1006. <https://doi.org/10.1130/G36989.1>

35. De Los Rios A, Wierzchos J, Ascaso C. The lithic microbial ecosystems of Antarctica's McMurdo Dry Valleys. *Antarct Sci.* 2014;25(5): 459-477. <https://doi.org/10.1017/S0954102014000194>

36. Friedmann EI, Hua M, Ocampo-Friedmann R. 3.6 Cryptoendolithic Lichen and Cyanobacterial Communities of the Ross Desert, Antarctica. *Polarforschung.* 1988;58:251-259. <https://hdl:10013/epic.29621.d001>

37. Friedmann EJ, Weed R. Abiotic Weathering in the Antarctic Cold Desert. *Science.* 1987;236(4802):703-705. <https://doi.org/10.1126/science.11536571>

38. Friedmann I. Endolithic Microorganisms in the Antarctic Cold Desert. *Science.* 1982;215(4536):1045-1053. <https://doi.org/10.1126/science.215.4536.1045>

39. Guglielmin M, Cannone N, Strini A, Lewkowicz AG. Biotic and abiotic processes on granite weathering landforms in a cryotic environment, Northern Victoria Land, Antarctica. *Permafrost Periglac Process.* 2005; 16(1):69-85. <https://doi.org/10.1002/ppp.514>

40. Johnston CG, Vestal JR. Biogeochemistry of oxalate in the antarctic cryptoendolithic lichen-dominated community. *Microb Ecol.* 1993; 25(3):305-319. <https://doi.org/10.1007/BF00171895>

41. Mergelov N, Mueller CW, Prater I, et al. Alteration of rocks by endolithic organisms is one of the pathways for the beginning of soils on Earth. *Sci Rep.* 2018;8(1):1-15. <https://doi.org/10.1038/s41598-018-21682-6>

42. Demirel-Floyd C, Elwood Madden AS, Soreghan GS, Elwood Madden ME. Determination of Inorganic Biosignatures Based on Terrestrial Analogs: Preliminary Results from Glacio-Fluvial Sediments from Iceland. In: 51st Lunar and Planetary Science Conference, Houston, Lunar and Planetary Institute; 2020 p. Abstract #2238. <http://www.lpi.usra.edu/meetings/lpsc2020/pdf/2238.pdf>

43. Hays LE, Graham HV, des Marais DJ, et al. Biosignature Preservation and Detection in Mars Analog Environments. *Astrobiology.* 2017; 17(4):363-400. <https://doi.org/10.1089/ast.2016.1627>

44. Montross SN, Skidmore M, Tranter M, Kivimäki AL, Parkes RJ. A microbial driver of chemical weathering in glaciated systems. *Geology.* 2013;41(2):215-218. <https://doi.org/10.1130/G33572.1>

45. Olsson-Francis K, Simpson AE, Wolff-Boenisch D, Cockell CS. The effect of rock composition on cyanobacterial weathering of crystalline basalt and rhyolite. *Geobiology.* 2012;10(5):434-444. <https://doi.org/10.1111/j.1472-4669.2012.00333.x>

46. Olsson-Francis K, Pearson VK, Steer ED, Schwennzer SP. Determination of Geochemical Bio-Signatures in Mars-Like Basaltic Environments. *Front Microbiol.* 2017;8:1668. <https://doi.org/10.3389/fmicb.2017.01668>

47. Welch SA, Ullman WJ. The effect of microbial glucose metabolism on bytownite feldspar dissolution rates between 5° and 35°C. *Geochim Cosmochim Acta.* 1999;63(19-20):3247-3259. [https://doi.org/10.1016/S0016-7037\(99\)00248-3](https://doi.org/10.1016/S0016-7037(99)00248-3)

48. Marra KR, Elwood Madden ME, Soreghan GS, Hall BL. BET surface area distributions in polar stream sediments: Implications for Silicate

Weathering in a Cold-Arid Environment. *Appl Geochem*. 2015;52: 31-42. <https://doi.org/10.1016/j.apgeochem.2014.11.005>

49. Marra KR, Soreghan GS, Elwood Madden ME, Keiser LJ, Hall BL. Trends in grain size and BET surface area in cold-arid versus warm-semiarid fluvial systems. *Geomorphology*. 2014;206:483-491. <https://doi.org/10.1016/j.geomorph.2013.10.018>

50. Ehlmann BL, Bish DL, Ruff SW, Mustard JF. Mineralogy and chemistry of altered Icelandic basalts : Application to clay mineral detection and understanding aqueous environments on Mars. *J Geophys Res*. 2012;117(E11):E0016. <https://doi.org/10.1029/2012JE004156>

51. Anderson SP. Glaciers show direct linkage between erosion rate and chemical weathering fluxes. *Geomorphology*. 2005;67(1-2):147-157. <https://doi.org/10.1016/j.geomorph.2004.07.010>

52. Anderson SP. Biogeochemistry of Glacial Landscape Systems. *Annu Rev Earth Planet Sci*. 2007;35(1):375-399. <https://doi.org/10.1146/annurev.earth.35.031306.140033>

53. Blott SJ, Croft DJ, Pye K, Saye SE, Wilson HE. Particle size analysis by laser diffraction. *Geol Soc Lond Spec Publ*. 2004;232(1):63-73. <https://doi.org/10.1144/GSL.SP.2004.232.01.08>

54. Brunauer S, Emmett PH, Teller E. Adsorption of Gases in Multi-molecular Layers. *J Am Chem Soc*. 1938;60(2):309-319. <https://doi.org/10.1021/ja01269a023>

55. Demirel C, McCollom N, Marra K, et al. Potential Biosignatures of Surface Alteration on Mars Inferred from Terrestrial Analog Regoliths. In: *Goldschmidt Abstracts*; 2019:769.

56. Bish DL, Howard SA. Quantitative phase analysis using the Rietveld method. *J Appl Cryst*. 1988;21(2):86-91. <https://doi.org/10.1107/S0021889887009415>

57. Demirel C, Soreghan GS, McCollom N, Elwood Madden AS, Marra K, Elwood Madden ME. XRD Characterization of Antarctic Glacial Drift Deposits: Implications for Quantifying Weathering Products on Earth and Mars. In: *49th Lunar and Planetary Science Conference, Houston, Lunar and Planetary Institute*; 2018 p. Abstract #1542. <http://www.lpi.usra.edu/meetings/lpsc2018/pdf/1542.pdf>

58. Eberl DD. User Guide to RockJock - A Program for Determining Quantitative Mineralogy from X-Ray Diffraction Data: 2003. <https://doi.org/10.3133/ofr200378>

59. Cornet L, Bertrand AR, Hanikenne M, Javaux EJ, Wilmette A, Baurain D. Metagenomic assembly of new (Sub)polar cyanobacteria and their associated microbiome from non-axenic cultures. *Microb Genom*. 2018;4(9):e000212. <https://doi.org/10.1099/mgen.0.000212>

60. Fernandez-Carazo R, Hodgson DA, Convey P, Wilmette A. Low cyanobacterial diversity in biotopes of the Transantarctic Mountains and Shackleton Range (80-82°S), Antarctica. *FEMS Microbiol Ecol*. 2011; 77(3):503-517. <https://doi.org/10.1111/j.1574-6941.2011.01132.x>

61. Rimstidt JD. *Geochemical Rate Models: An Introduction to Geochemical Kinetics*; Cambridge University Press; 2013.

62. Fiore MF, Moon DH, Tsai SM, Lee H, Trevors JT. Miniprep DNA isolation from unicellular and filamentous cyanobacteria. *J Microbiol Methods*. 2000;39(2):159-169. [https://doi.org/10.1016/S0167-7012\(99\)00110-4](https://doi.org/10.1016/S0167-7012(99)00110-4)

63. Li Y, Scales N, Blankenship RE, Willows RD, Chen M. Extinction coefficient for red-shifted chlorophylls: Chlorophyll d and Chlorophyll. *Biochim Biophys Acta Bioenerg*. 2012;1817(8):1292-1298. <https://doi.org/10.1016/j.bbabiobio.2012.02.026>

64. Meeks JC, Castenholz RW. Growth and photosynthesis in an extreme thermophile, *Synechococcus lividus* (Cyanophyta). *Arch Mikrobiol*. 1971;78(1):25-41. <https://doi.org/10.1007/BF00409086>

65. Fischer ER, Hansen BT, Nair V, Hoyt FH, Dorward DW. Scanning Electron Microscopy. *Curr Protoc Microbiol*. 2012;25(1):2B.2.1-2B.2.47. <https://doi.org/10.1002/9780471729259.mc02b02s25>

66. Kyle JE, Schroeder PA, Wiegel J. Microbial silicification in sinters from two terrestrial hot springs in the Uzon Caldera, Kamchatka, Russia. *Geomicrobiol J*. 2007;24(7-8):627-641. <https://doi.org/10.1080/01490450701672158>

67. Ramette A. Multivariate analyses in microbial ecology. *FEMS Microbiol Ecol*. 2007;62(2):142-160. <https://doi.org/10.1111/j.1574-6941.2007.00375.x>

68. Till R. *Statistical Methods for the Earth Scientist*. London: Macmillan Education UK; 1974.

69. Wackernagel H. *Multivariate Geostatistics*. Berlin, Heidelberg: Springer Berlin Heidelberg; 2003.

70. Benjamini Y, Krieger AM, Yekutieli D. Adaptive linear step-up procedures that control the false discovery rate. *Biometrika*. 2006;93(3): 491-507. <https://doi.org/10.1093/biomet/93.3.491>

71. Hirsch Peter, Gallikowski Claudia A., Siebert Jörg, Peissl Klaus, Kroppenstedt Reiner, Schumann Peter, Stackebrandt Erko, Anderson Robert. *Deinococcus frigens* sp. nov., *Deinococcus saxicola* sp. nov., and *Deinococcus marmoris* sp. nov., Low Temperature and Draught-tolerating, UV-resistant Bacteria from Continental Antarctica. *Systematic and Applied Microbiology*. 2004;27(6):636-645. <https://doi.org/10.1078/0723202042370008>

72. De Los Ríos A, Wierzchos J, Sancho LG, Ascaso C. Acid microenvironments in microbial biofilms of antarctic endolithic microecosystems. *Environ Microbiol*. 2003;5(4):231-237. <https://doi.org/10.1046/j.1462-2920.2003.00417.x>

73. Miller SR, Castenholz RW. Ecological Physiology of *Synechococcus* sp. Strain SH-94-5, a Naturally Occurring Cyanobacterium Deficient in Nitrate Assimilation. *Appl Environ Microbiol*. 2001;67(7):3002-3009. <https://doi.org/10.1128/AEM.67.7.3002-3009.2001>

74. Goldich SS. A Study in Rock-Weathering. *J Geol*. 1938;46(1):17-58. <http://www.jstor.org/stable/30079586>

75. Hall BL, Denton GH, Lux DR, Bockheim JG. Late Tertiary Antarctic Paleoclimate and Ice-Sheet Dynamics Inferred from Surficial Deposits in Wright Valley. *Geografiska Annaler Series a*. 1993;75(4):239-267. <https://doi.org/10.2307/521203>

76. Oddsson B, Gudmundsson MT, Edwards BR, Thordarson T, Magnússon E, Sigurðsson G. Subglacial lava propagation, ice melting and heat transfer during emplacement of an intermediate lava flow in the 2010 Eyjafjallajökull eruption. *Bull Volcanol*. 2016;78(7):48. <https://doi.org/10.1007/s00445-016-1041-4>

77. Wild B, Imfeld G, Guyot F, Daval D. Early stages of bacterial community adaptation to silicate aging. *Geology*. 2018;46(6):555-558. <https://doi.org/10.1130/G40283.1>

78. Shcolnick S, Keren N. Metal homeostasis in cyanobacteria and chloroplasts. Balancing Benefits and Risks to the Photosynthetic Apparatus. *Plant Physiol*. 2006;141(3):805-810. <https://doi.org/10.1104/pp.106.079251>

79. McKinley JP, Stevens TO, Westall F. Microfossils and paleoenvironments in deep subsurface basalt samples. *Geomicrobiol J*. 2000;17(1):43-54. <https://doi.org/10.1080/014904500270486>

80. Phillips-Lander CM, Harrold Z, Hausrath EM, et al. Snow Algae Preferentially Grow on Fe-containing Minerals and Contribute to the Formation of Fe Phases. *Geomicrobiol J*. 2020;37(6):572-581. <https://doi.org/10.1080/01490451.2020.1739176>

81. Frantz CM, Petryshyn VA, Corsetti FA. Grain trapping by filamentous cyanobacterial and algal mats: Implications for Stromatolite Microfabrics through Time. *Geobiology*. 2015;13(5):409-423. <https://doi.org/10.1111/gbi.12145>

82. Vincent WF, Gibson JAE, Pienitz R, et al. Ice shelf microbial ecosystems in the high arctic and implications for life on snowball earth. *Naturwissenschaften*. 2000;87(3):137-141. <https://doi.org/10.1007/s001140050692>

83. Ye Q, Tong J, Xiao S, et al. The survival of benthic macroscopic phototrophs on a Neoproterozoic snowball Earth. *Geology*. 2015;43(6): 507-510. <https://doi.org/10.1130/G36640.1>

84. Schulze-Makuch D, Irwin LN, Lipps JH, LeMone D, Dohm JM, Fairén AG. Scenarios for the evolution of life on Mars. *J Geophys Res E*. 2005;110(E12):1-12. <https://doi.org/10.1029/2005JE002430>

85. Kleinteich J, Wood SA, Küpper FC, et al. Temperature-related changes in polar cyanobacterial mat diversity and toxin production. *Nat Clim Chang.* 2012;2(5):356-360. <https://doi.org/10.1038/nclimate1418>

86. Shoenfelt EM, Winckler G, Annett AL, Hendry KR, Bostick BC. Physical Weathering Intensity Controls Bioavailable Primary Iron (II) Silicate Content in Major Global Dust Sources. *Geophys Res Lett.* 2019;46(19):10854-10864. <https://doi.org/10.1029/2019GL084180>

87. Andersen CB. Understanding Carbonate Equilibria by Measuring Alkalinity in Experimental and Natural Systems. *J Geosci Educ.* 2002; 50(4):389-403. <https://doi.org/10.5408/1089-9995-50.4.389>

88. Hoffman PF, Schrag DP. The snowball Earth hypothesis: testing the limits of global change. *Terra Nova.* 2002;14(3):129-155. <https://doi.org/10.1046/j.1365-3121.2002.00408.x>

89. Cannon KM, Mustard JF, Salvatore MR. Alteration of immature sedimentary rocks on Earth and Mars: Recording Aqueous and Surface-Atmosphere Processes. *Earth Planet Sci Lett.* 2015;417:78-86. <https://doi.org/10.1016/j.epsl.2015.02.017>

SUPPORTING INFORMATION

Additional supporting information may be found in the online version of the article at the publisher's website.

How to cite this article: Demirel-Floyd C, Soreghan GS, Madden MEE. Cyanobacterial weathering in warming periglacial sediments: Implications for nutrient cycling and potential biosignatures. *Permafrost and Periglac Process.* 2021; 1-15. doi:10.1002/ppp.2133